

## Stau-catalyzed $d$ - $t$ Nuclear Fusion

Koichi HAMAGUCHI<sup>1,2</sup>, Tetsuo HATSUDA<sup>1,3</sup>, Masayasu KAMIMURA<sup>3</sup>  
and Tsutomu T. YANAGIDA<sup>1,2</sup>

<sup>1</sup>*Department of Physics, The University of Tokyo, Tokyo 113-0033, Japan*

<sup>2</sup>*Institute for the Physics and Mathematics of the Universe,  
The University of Tokyo, Chiba 277-8568, Japan*

<sup>3</sup>*Theoretical Research Division, Nishina Center, RIKEN,  
Wako, Saitama 351-0198, Japan*

### Abstract

The gravitino of mass 10-100 GeV is a well motivated scenario in supergravity. If the stau is the next lightest supersymmetry particle, its life-time becomes order of  $10^{6-8}$  sec. If it is the case the stau makes a big impact on the nuclear fusion, since it is a charged particle. In this paper we perform a detailed calculation of a stau-catalyzed  $d$ - $t$  fusion. We find that if certain technical conditions are satisfied, it is not hopeless to use the nuclear fusion as a source of energy.

## §1. Introduction

The gravitino mass  $m_{3/2}$  is one of the most important parameter in supergravity, since it determines the scale of supersymmetry (SUSY) breaking. From the phenomenological point of view, the gravitino mass can be in the range from 1 eV to 100 TeV. The gravitino of mass  $O(10)$  GeV is particularly interesting, since it can be a dominant component of the DM in the universe<sup>1)</sup> and the thermal leptogenesis<sup>2)</sup> becomes consistent with cosmology if  $m_{3/2} \simeq 10 - 100$  GeV. If it is indeed the case, the next lightest SUSY particle (NLSP) has a long lifetime of order  $10^{6-8}$  sec. The most natural candidate of the NLSP is the bino-like neutralino or the scalar partner of the tau lepton stau ( $\tilde{\tau}$ ).<sup>\*)</sup> If the  $\tilde{\tau}$  is the NLSP and it has a long lifetime, it may give impact on the big bang nucleosynthesis and the nuclear fusion as a charged catalyst.<sup>\*\*)</sup> Effect of such negatively-charged and long-lived massive particle for the production of light elements in the big bang has been extensively studied (see e.g. the review, Ref.10).) Also, three of the present authors (K.H, T.H. and T.T.Y.) have discussed the effects of long-lived  $\tilde{\tau}$  on the  $d-d$  nuclear fusion as a possible energy source.<sup>11)</sup> Advantages as well as (serious) problems of the  $d-d$  and  $d-t$  fusion catalyzed by massive charged particles have been also discussed before<sup>12),13)</sup> in analogy with the muon catalyzed fusion.

The purpose of this paper is to present a detailed quantum three-body calculation of the  $\tilde{\tau}$ -catalyzed  $d-t$  nuclear fusion,  $\tilde{\tau} + d + t \rightarrow \alpha + n + \tilde{\tau}$ , especially its fusion rate and the sticking probability. Although it is certainly necessary to develop new technology to make such catalyzed fusion as a new source of energy, the present calculation would give one of the basis for such development.

Note that the following discussion is model-independent and applicable to any heavy charged particle with a sufficiently long lifetime. For instance, charged Wino NLSP can have a long lifetime if its mass is degenerate with the neutral Wino LSP. (See Ref. 14) for candidates for charged massive particles in various particle physics models beyond the Standard Model.) Thus, the “stau” in the following analysis can be replaced with any long-lived charged particle.

---

<sup>\*)</sup> The above scenario is well realized in gauge mediation of SUSY breaking. It is remarkable that the Higgs boson mass around 125 GeV suggested in the recent report of the LHC experiments<sup>3),4)</sup> can be easily explained if one considers the Higgs-messenger mixing<sup>5)</sup> or extra matters<sup>6)</sup> in gauge mediation models. The latest LHC result has placed a lower bound on the stau mass as  $m_{\tilde{\tau}} \gtrsim 221$  GeV.<sup>7)</sup>

<sup>\*\*)</sup> The stau decay may also destroy the success of BBN. The cosmological problems caused by the catalysis, and by the stau decay, can be solved by a late-time entropy production<sup>8)</sup> or an enhanced coupling of stau to Higgs boson<sup>9)</sup> in the SUSY standard model.

## §2. Outline of the stau-catalyzed fusion in D-T mixture

Let us first outline how the  $d$ - $t$  fusion catalyzed by  $\tilde{\tau}$  proceeds inside the D-T mixture with a wide range of temperature  $10 \text{ K} \lesssim T \lesssim 1000 \text{ K}$ . Suppose that a free  $\tilde{\tau}$  is stopped in the D-T mixture, and the formation of the 1s state of the  $\tilde{\tau}t$  and  $\tilde{\tau}d$  atom occurs through the capture process to the higher orbit,  $\tilde{\tau} + (te^-) \rightarrow (\tilde{\tau}t) + e^-$  and  $\tilde{\tau} + (de^-) \rightarrow (\tilde{\tau}d) + e^-$ , followed by the de-excitation to their 1s states.\*)

The basic  $d$ - $t$  fusion reaction is

$$d + t \rightarrow \alpha + n \quad (Q = 17.6 \text{ MeV}). \quad (2.1)$$

The reaction rate of this process is enhanced by the charge neutral  $\tilde{\tau}t$  and  $\tilde{\tau}d$  bound states in D-T mixture through the catalyzed processes

$$(\tilde{\tau}t)_{1s} + d \rightarrow \alpha + n + \tilde{\tau}, \quad (2.2)$$

$$(\tilde{\tau}d)_{1s} + t \rightarrow \alpha + n + \tilde{\tau}. \quad (2.3)$$

Essential mechanism of the  $\tilde{\tau}$  catalyzed fusion is similar to the muon catalyzed fusion: the long range Coulomb barrier is screened by the formation of neutral bound states tabulated in Table I. Moreover, due to the large  $\tilde{\tau}$  mass ( $> 100 \text{ GeV}$ ) and small size (15 fm or less) of  $\tilde{\tau}t$  and  $\tilde{\tau}d$ , the short range Coulomb repulsion is screened and even turns into an attraction which does not happen in the case of  $\mu$ -catalyzed fusion where  $\mu t$  and  $\mu d$  have a large size of about 250 fm. We will show in the later sections by the fully quantum mechanical three-body calculations that the reaction rates of (2.2) and (2.3) are enhanced and the averaged reaction rate  $\lambda_f$  becomes  $2.6 \times 10^8 \text{ s}^{-1}$  independent of the temperature of the D-T mixture under consideration.

In the above reactions, there is always a possibility of forming  $\tilde{\tau}\alpha$  bound states in the final state. Once such a sticking process takes place, stucked  $\tilde{\tau}$  can no longer be used as a catalyzer, so that the catalyzed fusion process is eventually stopped by the sticking. We calculate this sticking probability to be  $\bar{\omega}_s = 1.5 \times 10^{-3}$  as shown later, so that the energy product per  $\tilde{\tau}$  is estimated as  $Q/\bar{\omega}_s \simeq 12 \text{ GeV}$ .

## §3. Model and method

Before entering the stau-catalyzed three-body reactions (2.2) and (2.3), we first calculate the cross section of the standard reaction (2.1) by taking the same three-body calculation

---

\*) Note that there is no three-body bound state of  $(\tilde{\tau}dt)$ , which we have checked explicitly by a three-body calculation. This is different from the case of  $\tilde{\tau}$ - $d$ - $d$  system discussed in Ref. 11). Stau-catalyzed fusions in  $\tilde{\tau}$ - $d$ - $d$  system will be briefly discussed in Sec. 4.

System	$\mu_r$	$a_B$	$E_b$
$\mu d$	0.1 GeV	270 fm	2.7 keV
$\mu t$	0.1 GeV	270 fm	2.7 keV
$\tilde{\tau} d$	1.9 GeV	15 fm	50 keV
$\tilde{\tau} t$	2.8 GeV	10 fm	74 keV

Table I. Reduced mass  $\mu_r$ , Bohr radius  $a_B$  and binding energy of the 1s state for muonic and stau atoms (for stau mass 200 GeV).

method of Refs. 15), 16) in which the fully-quantum method was applied systematically to the various types of stau-catalyzed big-bang nucleosynthesis reactions. We explicitly follow §4 of Ref. 16) on three-body breakup reactions. We do not explicitly treat the complicated channel coupling between the entrance and exit channels. Instead, we employ an alternative model which is easy to incorporate into the calculation of the three-body processes (2·2) and (2·3). Namely, we take into account the entrance  $d$ - $t$  channel alone and introduce a complex potential  $V_{d-t}(r)$  between  $d$  and  $t$ :

$$V_{d-t}^{\text{nucl}}(r) = V_{d-t}^{\text{(real)}}(r) + iV_{d-t}^{\text{(imag)}}(r) \quad (3\cdot1)$$

as seen in nuclear optical-model potentials. Since there are no other open channel than the entrance and exit channels in (2·1) at the energies concerned here, the absorption cross section due to the imaginary potential represents the reaction cross section to the exit  $\alpha + n$  channel. We determine the potential  $V_{d-t}^{\text{nucl}}(r)$  so as to reproduce the observed cross section ( $S$ -factor) of (2·1) at low energies ( $\lesssim 1$  MeV).

Next, we incorporate this complex potential  $V_{d-t}^{\text{nucl}}(r)$  into the three-body Hamiltonian of the  $d + t + \tilde{\tau}$  system (Fig. 1) with obvious notation,

$$H = -\frac{\hbar^2}{2m_c} \nabla_{\mathbf{r}_c}^2 - \frac{\hbar^2}{2M_c} \nabla_{\mathbf{R}_c}^2 + V_{t-\tilde{\tau}}^{\text{coul}}(r_1) + V_{d-\tilde{\tau}}^{\text{coul}}(r_2) + V_{d-t}^{\text{coul}}(r_3) + V_{d-t}^{\text{nucl}}(r_3), \quad (3\cdot2)$$

where the kinetic-energy operator is equivalent for  $c = 1 - 3$ . We solve the Schrödinger equation  $(H - E_{\text{total}})\Psi_{JM} = 0$  for the elastic scattering between  $\tilde{\tau}t$  and  $d$  and that between  $\tilde{\tau}d$  and  $t$ . The absorption cross section obtained in this scattering calculation is considered to give the reaction cross section of the stau-catalyzed reactions (2·2) and (2·3).

In the following, we explain our method taking the case of  $\tilde{\tau}t + d$  reaction on  $c = 1$  (similarly for the  $\tilde{\tau}d + t$  on  $c = 2$ ). The total wave function with the angular momentum  $J$  and its  $z$ -component  $M$  is written as

$$\Psi_{JM} = \phi_{1s}^{(1)}(\mathbf{r}_1) \chi_{JM}^{(1)}(\mathbf{R}_1) + \Phi_{JM}^{(\text{corr.})}, \quad (3\cdot3)$$

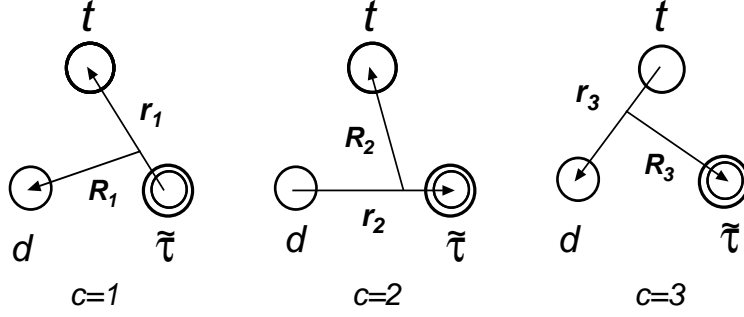


Fig. 1. Three sets of Jacobi coordinates in the  $d + t + \tilde{\tau}$  system. The scattering channels  $\tilde{\tau}t + d$  and  $\tilde{\tau}d + t$  are described by using the coordinate systems  $c = 1$  and  $c = 2$ , respectively. The coordinate  $c = 3$  is responsible for describing the strong nuclear correlation and the nuclear fusion.

where  $\phi_{1s}^{(1)}(\mathbf{r}_1)$  represents the  $1s$  wave function of the  $\tilde{\tau}d$  atom and  $\chi_{JM}^{(1)}(\mathbf{R}_1)$  for the  $(\tilde{\tau}d)_{1s} + d$  scattering wave. The scattering boundary condition imposed on  $\chi_{JM}^{(1)}(\mathbf{R}_1) (\equiv \chi_J^{(1)}(R_1) Y_{JM}(\hat{\mathbf{R}}_1))$  is given by

$$\lim_{R_1 \rightarrow \infty} R_1 \chi_J^{(1)}(R_1) = u_J^{(-)}(k_1, R_1) - S_{1 \rightarrow 1}^J u_J^{(+)}(k_1, R_1), \quad (3.4)$$

where  $u^{(-)}$  and  $u^{(+)}$  are the asymptotic incoming and outgoing wave function, and  $\hbar^2 k_1^2 / 2M_1 = E_{\text{total}} - E_{1s}^{(1)} \equiv E$ ,  $E_{1s}^{(1)}$  being the energy of  $(\tilde{\tau}d)_{1s}$ .

The second term of (3.3),  $\Phi_{JM}^{(\text{corr.})}$ , is introduced to describe the short-range correlation along the coordinate  $\mathbf{r}_3$  due to the strong nuclear interaction  $V_{d-t}^{\text{nucl}}(\mathbf{r}_3)$ ; the correlation amplitude is not included in the first scattering term, but plays an important role in the  $d$ - $t$  fusion process. Since  $\Phi_{JM}^{(\text{corr.})}$  is asymptotically vanishing amplitude, it is expanded in terms of three-body Gaussian basis functions<sup>17)</sup> as

$$\Phi_{JM}^{(\text{corr.})} = \sum_{nl, NL} b_{nl, NL} [\phi_{nl}(\mathbf{r}_3) \psi_{NL}(\mathbf{R}_3)]_{JM}, \quad (3.5)$$

$$\phi_{nlm}(\mathbf{r}) = r^l e^{-(r/r_n)^2} Y_{lm}(\hat{\mathbf{r}}), \quad \psi_{NLM}(\mathbf{R}) = R^L e^{-(R/R_N)^2} Y_{LM}(\hat{\mathbf{R}}), \quad (3.6)$$

where the Gaussian ranges are postulated to lie in a geometric progression:

$$r_n = r_{\min} a^{n-1}, \quad (n = 1 - n_{\max}) \quad R_N = R_{\min} A^{N-1}. \quad (N = 1 - N_{\max}) \quad (3.7)$$

After solving the Schrödinger equation to determine  $S_{1 \rightarrow 1}^J$  and  $b_{nl, NL}$ ,<sup>17), 16)</sup> we derive the absorption cross section by

$$\sigma(E) = \frac{\pi}{k_1^2} \sum_{J=0}^{\infty} (2J+1) (1 - |S_{1 \rightarrow 1}^J|^2). \quad (3.8)$$

This absorption cross section is alternatively expressed as

$$\sigma(E) = \frac{-2}{\hbar v_1} \langle \Psi_{JM} | V_{d-t}^{(\text{imag})}(r_3) | \Psi_{JM} \rangle, \quad (3.9)$$

where  $v_1$  is the c.m. velocity of the incident channel ( $c = 1$ ). It is to be noted that the two equivalent  $\sigma(E)$  utilize information from quite different parts of the three-body wave function  $\Psi_{JM}$ , namely, the information from the asymptotic part along  $\mathbf{R}_1$  in the former expression and that from the internal part along  $\mathbf{r}_3$  in the latter. Therefore, it is a severe test of the numerical accuracy of the three-body calculation to examine the agreement between the two types of  $\sigma(E)$ . In our calculation below, we obtained a precise agreement between their numbers in four significant figures.

The reaction rate  $\langle \sigma v \rangle$  at temperature  $T$  is expressed as

$$\langle \sigma v \rangle = (8/\pi M_1)^{1/2} (kT)^{-3/2} \int_0^\infty \sigma(E) e^{-E/kT} dE, \quad (3.10)$$

where  $k$  is the Boltzmann constant. It is noted here that if, as we shall meet below,  $\sigma(E) \propto 1/\sqrt{E}$ , then the rate  $\langle \sigma v \rangle$  becomes independent of temperature  $T$ .

## §4. Calculated results

### 4.1. Interactions

As for the complex potential  $V_{d-t}^{\text{nucl}}(r)$ , we take the same one as used in the study of muon catalyzed  $d-t$  fusion in Ref. 18), where the fusion rate and the  $\alpha\mu$  sticking probability in the  $dt\mu$  molecule were calculated using  $V_{d-t}^{\text{nucl}}(r)$  having the Woods-Saxon shape with five different types of parameter sets. Since the calculated results did not significantly depend on the sets (all reproduce the cross section of (2.1) very well for  $E_{\text{c.m.}} \lesssim 1$  MeV), we here employ a parameter set:  $\{V_0 = -38.0$  MeV,  $R_0 = 3.0$  fm,  $a_0 = 0.5$  fm $\}$  for the real part and  $\{W_0 = -0.37$  MeV,  $R_I = 3.0$  fm,  $a_I = 0.5$  fm $\}$  for the imaginary part. The Coulomb potential between  $d$  and  $t$  is constructed by assuming the Gaussian shape of the charge distribution of  $d(t)$  which reproduces observed r.m.s. radius.

Coulomb and nuclear potential between  $\tilde{\tau}t$  and  $d$  (between  $\tilde{\tau}d$  and  $t$ ) are obtained by folding the Coulomb and nuclear  $d-t$  potentials into the triton (deuteron) density of the  $1s$ -state of the  $\tilde{\tau}t$  ( $\tilde{\tau}d$ ) atom. In Fig. 2, we illustrate the case of the  $\tilde{\tau}t-d$  potential. The Coulomb  $\tilde{\tau}-d$  potential is given by the dashed line. The dotted line is the  $d-t$  folded part of the Coulomb  $\tilde{\tau}t-d$  potential. The thick solid line is sum of these two Coulomb potentials, which almost vanishes for  $R_1 \gtrsim 20$  fm. The thin solid line is the real part of the folded nuclear  $\tilde{\tau}t-d$  potential. The imaginary part (not illustrated) has the same shape of the real part but is  $-0.01$  MeV at  $R_1 = 0$ .

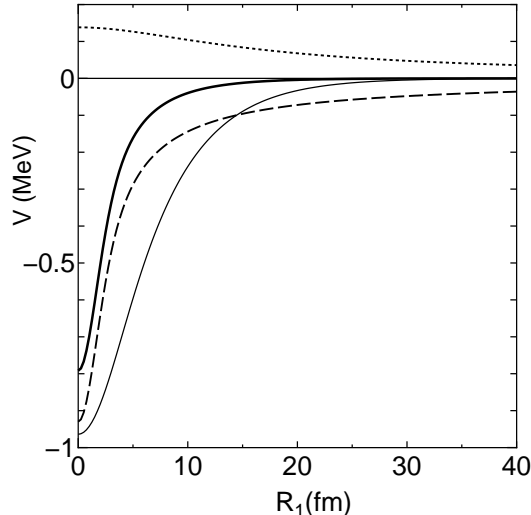


Fig. 2. Coulomb and nuclear potential between  $(\tilde{\tau}t)_{1s}$  and  $d$  as a function of the coordinate  $R_1$  in Fig. 1 ( $m_{\tilde{\tau}} \gg m_t$ ). They are obtained by folding the  $d$ - $t$  potential into the triton density in the  $(\tilde{\tau}d)_{1s}$  atom except for the Coulomb  $\tilde{\tau}$ - $d$  potential by the dashed line. The dotted line is the  $d$ - $t$  folded part of the Coulomb  $\tilde{\tau}$ - $d$  potential. The thick solid line is sum of these two Coulomb potentials. The thin solid line is the real part of the folded nuclear  $\tilde{\tau}$ - $t$ - $d$  potential.

The screened Coulomb potential (thick solid line) is attractive everywhere. The folded nuclear potential is more attractive than this Coulomb potential. Moreover,  $t$  in  $\tilde{\tau}t$  ( $d$  in  $\tilde{\tau}d$ ) is moving with an averaged kinetic energy of 72 keV (48 keV). We can thus expect a huge enhancement of the fusion reaction rate at low energies compared with the bare  $d$ - $t$  fusion and the muon-catalyzed  $d$ - $t$  fusion-in-flight of the  $d$ - $t\mu$  and  $t$ - $d\mu$  systems.\*)

Therefore, it is of particular importance to describe properly the short-range  $d$ - $t$  relative motion at the moment of the fusion. This is not satisfactorily done by the first scattering term of (3-3) since it does not explicitly include the  $d$ - $t$  coordinate ( $\mathbf{r}_3$ ), but is well realized by the second term,  $\Phi_{JM}^{(\text{corr.})}$ , using the basis functions  $\phi_{nl}(\mathbf{r}_3)$  along the  $d$ - $t$  coordinate. We took the Gaussian parameters as  $\{n_{\text{max}} = 10; r_{\text{min}} = 0.2 \text{ fm}, r_{\text{max}} = 10.0 \text{ fm}\}$  for  $\phi_{nl}(\mathbf{r}_3)$  and  $\{N_{\text{max}} = 15; R_{\text{min}} = 1.0 \text{ fm}, R_{\text{max}} = 50.0 \text{ fm}\}$  for  $\psi_{NL}(\mathbf{R}_3)$ . But, we found in the actual calculations below that  $l = L = J = 0$  is sufficient for the low energies ( $E \lesssim 10^1 \text{ eV}$ ) concerned in the present paper.

We assume infinitely heavy stau. However, as studied in Ref.16), results of the stau-catalyzed reaction are known to depend little (by a few percents) on the mass of stau ( $\gtrsim 100$

---

\*) In the  $d + t + \mu$  system, the  $d$ - $t$  Coulomb barrier at short range is not screened by muon (the muon Bohr radius is some 250 fm); this can be understood, in Fig. 3, by changing the sign of the two Coulomb potentials in the dashed and dotted lines. Furthermore, the kinetic energy of  $d$  in  $d\mu$  ( $t$  in  $t\mu$ ) is negligibly small compared with that of  $d$  in  $\tilde{\tau}d$  ( $t$  in  $\tilde{\tau}t$ ).

GeV) except for the case of specific resonant reactions.

#### 4.2. Fusion rate

We calculated the reaction (absorption) cross section  $\sigma(E)$  of the  $\tilde{\tau}t + d$  reaction (2.2) for the energy region of  $10^{-4}$  eV  $\lesssim E \lesssim 10^2$  eV (we are particularly interested in  $10$  K  $\lesssim T \lesssim 1000$  K, namely,  $10^{-3}$  eV  $\lesssim E \lesssim 10^{-1}$  eV). We found that contribution from  $J > 0$  is negligible and the cross section is well represented by

$$\sigma_{\tilde{\tau}t+d}(E) = 1.2 \times 10^{-20} / \sqrt{E(\text{eV})} \text{ cm}^2, \quad (4.1)$$

which follows the usual  $1/v$ -law for low energy reactions with a neutral-charge particle (here  $\tilde{\tau}d$ ).\*) With the  $E$ -dependence of the cross section in (4.1), the rate  $\langle \sigma v \rangle$  for the  $\tilde{\tau}t + d$  reaction (2.2) is expressed independently of  $T$ , for  $kT \lesssim 10^1$  eV, as

$$\langle \sigma v \rangle_{\tilde{\tau}t+d} = 9.7 \times 10^{-15} \text{ cm}^3 \text{ s}^{-1}. \quad (4.2)$$

Similarly, the reaction cross section of the  $\tilde{\tau}d + t$  reaction (2.3) is obtained as

$$\sigma_{\tilde{\tau}d+t}(E) = 2.5 \times 10^{-21} / \sqrt{E(\text{eV})} \text{ cm}^2 \quad (4.3)$$

for  $E \lesssim 10^2$  eV. The reaction rate  $\langle \sigma v \rangle_{\tilde{\tau}d+t}$  is expressed, for  $kT \lesssim 10^1$  eV, as\*\*)

$$\langle \sigma v \rangle_{\tilde{\tau}d+t} = 2.4 \times 10^{-15} \text{ cm}^3 \text{ s}^{-1}. \quad (4.4)$$

From the results (4.2) and (4.4), we can say that, for temperature  $T \lesssim 10^5$  K, the stau-catalyzed  $d$ - $t$  fusion occurs with the *same* rate at any  $T$ . For the density  $n \simeq 4.25 \times 10^{22}$  atoms/cm<sup>3</sup>, irrespective of gas-, liquid- and solid-phases of the D-T mixture, the above reaction rates lead to  $\lambda_f \simeq n \langle \sigma v \rangle \simeq 2.6 \times 10^8 \text{ s}^{-1}$ , independently of temperature, on the average of (4.2) and (4.4).

The formation rate of the  $1s$  state of the  $\tilde{\tau}t$  ( $\tilde{\tau}d$ ) atom in the D-T mixture is expected to be much faster than the above fusion rate. Then, the cycling rate,  $\lambda_c$ , of the stau-catalyzed fusion is given by  $\lambda_c \simeq 2.6 \times 10^8 \text{ s}^{-1}$ , which is compatible with the the largest  $\lambda_c$  achieved so far in the muon-catalyzed  $d$ - $t$  fusion experiment. The time scale of the one cycle is given by  $1/\lambda_c = 3.8 \times 10^{-9}$  sec.

---

\*) If we omit, in (3.3), the second term  $\Phi_{JM}^{(\text{corr.})}$  for describing the strong  $d$ - $t$  nuclear correlation along  $\mathbf{r}_3$ , the cross section becomes smaller by one order.

\*\*\*) If we employ another (longer-ranged) set of nuclear interaction in Ref.16), namely  $\{V_0 = -16.0 \text{ MeV}, R_0 = 5.0 \text{ fm}, a_0 = 0.3 \text{ fm}\}$  for the real part and  $\{W_0 = -0.28 \text{ MeV}, R_I = 2.5 \text{ fm}, a_I = 0.3 \text{ fm}\}$  for the imaginary part, we obtain  $\langle \sigma v \rangle_{\tilde{\tau}t+d} = 2.0 \times 10^{-15} \text{ cm}^3 \text{ s}^{-1}$  and  $\langle \sigma v \rangle_{\tilde{\tau}d+t} = 9.5 \times 10^{-15} \text{ cm}^3 \text{ s}^{-1}$ , which is close to the result in (4.2) and (4.4), respectively.

### 4.3. Sticking probability

In the exit channel of the fusion reactions (2.2) and (2.3), some fraction of the  $\alpha$  particles may be trapped by  $\tilde{\tau}$  and form a Coulomb bound state  $\tilde{\tau}\alpha$ , though most of them escape into the  $\tilde{\tau}\alpha$  continuum states. If this  $\tilde{\tau}\alpha$ -sticking process happens, the fusion chain will be terminated. The probability of sticking to the bound states gives a stringent constraint on the number of fusion reactions per  $\tilde{\tau}$ . For the muon-catalyzed fusion, the sticking probability is known to be about 1% (15%) for  $dt\mu$  ( $dd\mu$ ).

In the sudden approximation where the instantaneous  $dt$  fusion does not affect the states of infinitely heavy  $\tilde{\tau}$ , the sticking probability for the fusion-in-flight may be estimated from an overlap integral of the initial and final state wave functions in the same manner of the sticking after fusion in the  $dt\mu$  ( $dd\mu$ ) molecule: \*)

$$\omega_s = \sum_f^{\text{bound}} \omega_{s,f}, \quad (4.5)$$

$$\omega_{s,f} = \frac{|\langle \phi_f(\mathbf{r}) \exp(i\mathbf{k}_f \cdot \mathbf{r}) | \Phi_i(\mathbf{r}) \rangle|^2}{|\langle \Phi_i(\mathbf{r}) | \Phi_i(\mathbf{r}) \rangle|^2}, \quad (4.6)$$

where  $\Phi_i(\mathbf{r})$  is the initial scattering wave function (3.3) at the instant of fusion ( $r_3 = 0$ ):

$$\Phi_i(\mathbf{r}) = \Psi_{JM}(r_3 = 0, \mathbf{R}_3 = \mathbf{r}) = \phi_{00}^{(1)}(\mathbf{r}) \chi_{JM}^{(1)}(\mathbf{r}) + \Phi_{JM}^{(\text{corr.})}(r_3 = 0, \mathbf{R}_3 = \mathbf{r}), \quad (4.7)$$

and  $\phi_f(\mathbf{r})$  denotes a normalized final state  $(\tilde{\tau}\alpha)_f$  and  $\mathbf{k}_f$  is the wave vector of the relative motion between  $n$  and  $\tilde{\tau}\alpha$  determined by the relation  $\hbar^2 k_f^2 / 2m_n + E_f = 17.6$  MeV. The summation in (4.5) is over all the *bound* states  $(\tilde{\tau}\alpha)_f$  (we have  $\omega_s = 1$  if the summation is taken over all the  $\tilde{\tau}\alpha$  states including the continuum).

Calculated  $\tilde{\tau}\alpha$ -sticking probability  $\omega_s$  and its partial components  $\omega_{s,f}$  are listed in Table II for the reactions (2.2) and (2.3).\*\*) If we average the two values of  $\omega_s$  taking the magnitude

---

\*) For the fusion-in-flight, the sticking probability is derived as follows according to the reaction theory (see Ref. 19) for more details): In the reaction (2.2), we consider that the  $d$  and  $\alpha$  are composed of  $n + p$  and  $t + p$ , respectively, and  $p$  in  $d$  is transferred to  $t$  to form  $\alpha$ . The transition matrix  $T_f$  to the final state  $f$  in the  $\tilde{\tau}\alpha$  atom is exactly expressed with the obvious notation as

$$T_f = \langle \psi_\alpha(\mathbf{r}_{tp}) \phi_f(\mathbf{r}_{\tilde{\tau}\alpha}) \exp(i\mathbf{k}_f \cdot \mathbf{r}_{\tilde{\tau}n}) | V_{nt}(\mathbf{r}_{nt}) + V_{np}(\mathbf{r}_{np}) | \Psi_{\text{scatt.}}^{\text{exact}} \rangle,$$

where  $\Psi_{\text{scatt.}}^{\text{exact}}$  is the exact wave function of the reaction (2.2). If we assume  $V_{nt}(\mathbf{r}_{nt}) \propto \delta(\mathbf{r}_{nt})$ ,  $V_{np}(\mathbf{r}_{np}) \propto \delta(\mathbf{r}_{np})$  and  $\psi_\alpha(\mathbf{r}_{tp}) \propto \delta(\mathbf{r}_{tp})$ , which leads to  $\mathbf{r}_{\alpha n} = 0$  and  $\mathbf{r}_{\tilde{\tau}n} = \mathbf{r}_{\tilde{\tau}\alpha} (\equiv \mathbf{r})$ , and replace  $\Psi_{\text{scatt.}}^{\text{exact}}$  by our  $\Psi_{JM}$  in (3.3), we then obtain  $T_f \propto \langle \phi_f(\mathbf{r}) \exp(i\mathbf{k}_f \cdot \mathbf{r}) | \Phi_i(\mathbf{r}) \rangle$ , which is used in (4.6).

\*\*) If we employ another set of nuclear interaction that was mentioned in one of the previous footnotes, we obtain the sticking probability  $\omega_s \simeq 1.4 \times 10^{-3}$  ( $1.8 \times 10^{-3}$ ) for the  $\tilde{\tau}t + d$  ( $\tilde{\tau}d + t$ ) reaction, which is the same as the result in Table II.

Even if we omit, in (3.3), the second term  $\Phi_{JM}^{(\text{corr.})}$  for describing the strong  $d$ - $t$  nuclear correlation along  $\mathbf{r}_3$ , the sticking probability  $\omega_{s,f}$  does not change significantly since the second term works to increase much the cross section but almost equally for all the final states.

Table II. Calculated  $\tilde{\tau}\alpha$ -sticking probability  $\omega_s$  and its partial components  $\omega_{s,f}$ .

reaction	$\omega_{s,f}$				$\omega_s$
	1s	2s	2p	others	total
$\tilde{\tau}t + d$	$1.1 \times 10^{-3}$	$1.8 \times 10^{-4}$	$4.1 \times 10^{-6}$	$1.1 \times 10^{-4}$	$1.4 \times 10^{-3}$
$\tilde{\tau}d + t$	$1.4 \times 10^{-3}$	$2.4 \times 10^{-4}$	$5.3 \times 10^{-6}$	$1.5 \times 10^{-4}$	$1.8 \times 10^{-3}$

of the reaction rates (4.2) and (4.4) as averaging weight, we have  $\bar{\omega}_s = 1.5 \times 10^{-3}$ . This is several times smaller than  $\omega_s (\simeq 0.01)$  in the muon-catalyzed  $d$ - $t$  fusion in the  $dt\mu$  molecule.

The sticking probability listed in Table II does not depend on the energy (for  $E \lesssim 10^1$  eV) concerned in this paper. This is because of the following reason: Integration up to only  $r \simeq 15$  fm contributes to the numerator of Eq. (4.6). In this region, as seen in Fig. 2, the incident energy is negligibly small compared with the depth of the attractive Coulomb and nuclear potentials.

Since the number of fusion cycles available before terminating due to the sticking loss of  $\tilde{\tau}$  is given by  $1/\bar{\omega}_s$  (assuming no reactivation of stucked  $\tilde{\tau}$ ), the energy product  $E_{\tilde{\tau}dt}$  per  $\tilde{\tau}$  is estimated as

$$E_{\tilde{\tau}dt} = \frac{17.6 \text{ MeV}}{1.5 \times 10^{-3}} \simeq 12 \text{ GeV}. \quad (4.8)$$

#### 4.4. *stau-catalyzed d-d fusion*

Here we shortly comment on the stau-catalyzed  $d$ - $d$  fusion. It is much less effective than the stau-catalyzed  $d$ - $t$  fusion studied above. The reason is as follows: Differently from the  $d$ - $t$  case, the  $\tilde{\tau} + d + d$  system has a bound state, the  $(\tilde{\tau}dd)_{J=0}$  atom, at 2.8 keV below the  $(\tilde{\tau}d)_{1s} + d$  threshold. However, since there is no excited bound state, we cannot expect a rapid formation of the  $(\tilde{\tau}dd)_{J=0}$  atom via the Vesman's resonant mechanism<sup>20)</sup> (a bound state shallower than 4.5 eV is required). Moreover, the sticking probability after the fusion in the atom is  $\omega_s \simeq 0.03$ . As for the stau-catalyzed  $d$ - $d$  fusion-in-flight, the sticking probability is  $\omega_s \simeq 0.02$ , whereas the Q-value is about 3.7 MeV (average of  $Q = 3.3$  MeV for  $d+d \rightarrow n+{}^3\text{He}$  and  $Q = 4.0$  MeV for  $d+d \rightarrow p+t$ ). Thus, the energy product  $E_{\tilde{\tau}dd}$  per  $\tilde{\tau}$  is estimated to be  $E_{\tilde{\tau}dd} \simeq 3.7 \text{ MeV}/0.02 \simeq 0.15 \text{ GeV}$  (assuming no reactivation of stucked  $\tilde{\tau}$ ), which is much smaller than  $E_{\tilde{\tau}dt} \simeq 12 \text{ GeV}$ .

## §5. Discussion

Let us now briefly discuss a possible production of the staus in the laboratory. We consider the  $\mu + N$  (nucleon) scattering with a fixed nuclear target. The stau-production cross section depends on the spectrum of SUSY particles. In order to have an optimistic estimate of the number of produced stau, let us estimate the slepton-production cross section by using the sparticle production cross section in cosmic ray neutrino-nucleon scattering studied e.g., in Ref. 21). For the neutrino energy  $E_\nu \simeq 2000$  TeV, for the SUSY model point SPS 7,<sup>22)\*</sup> the cross section is  $\mathcal{O}(10^{-38} \text{ cm}^2)$ .<sup>21)</sup> Since all SUSY particles decay quickly to the staus, the stau-production cross section is also of  $\mathcal{O}(10^{-38} \text{ cm}^2)$ . Thus, assuming a laboratory energy of the muon  $E_\mu \simeq \mathcal{O}(1000)$  TeV, and by further assuming a Fe target of  $\mathcal{O}$  (km) length with the nucleon density  $n_N \simeq 5 \times 10^{24}/\text{cm}^3$ , the number of produced staus per muon is estimated to be  $\mathcal{O}(10^{-8})$ . This implies that we need at least  $10^8 \times 1000$  TeV ( $10^{14}$  GeV) to produce a single stau.<sup>\*\*)</sup> On the other hand, one stau could reproduce  $\simeq 12$  GeV energy for a single chain (namely,  $1/\omega_s$  cycles) of the  $d$ - $t$  fusion as we have discussed in §3. Therefore, to make the present stau-catalyzed  $d$ - $t$  fusion to be of practical use, we need to recycle the stau at least  $10^{13}$  times, even if the above optimistic estimate holds. For the recycling, we should collect the inactive  $\tilde{\tau}\alpha$  atoms and strip the  $\alpha$  particle from the stau. It is beyond the scope of the present paper to investigate possible reactivation mechanisms.

As shown in §4.2, the time scale of the one cycle of the stau-catalyzed  $d$ - $t$  fusion is  $3.8 \times 10^{-9}$  sec. This leads to the time scale of a single chain which is estimated as  $3.8 \times 10^{-9} \text{ sec}/(1.5 \times 10^{-3}) = 2.5 \times 10^{-6}$  sec. Assuming that we find a sufficiently fast reactivation mechanism of stau, the lifetime of the stau should be longer than  $2.5 \times 10^{-6} \text{ sec} \times 10^{13} = 2.5 \times 10^7 \text{ sec} \simeq 300$  days at least for the output energy to exceed the input energy. In order to make the present stau-catalyzed nuclear fusion an interesting source of energy, we thus need to find a more efficient mechanism and/or technology for the stau production.

Other than catalyzing the nuclear  $d$ - $t$  fusion, negatively charged  $\tilde{\tau}$  may also provide a new tool in nuclear physics. Indeed, if the  $\tilde{\tau}$  is embedded in heavy nuclei, it will form exotic Coulomb bound states with their level structures affected by the charge distribution of the nuclear interior. Namely, the long-lived stau may be used as a probe of the deep interior of heavy nuclei.

---

\*) This model point is already excluded by the LHC,<sup>23)</sup> but we use it just for illustration.

\*\*) This is, of course, an overoptimistic guesstimate. It will cost much more than 1000 TeV to create a 1000 TeV muon, and it will not be easy to capture all the high-energy staus produced.

## Acknowledgement

This work was supported by Grand-in-Aid for Scientific research from the Ministry of Education, Science, Sports, and Culture (MEXT), Japan, No. 21740164 (K.H.), and No. 22244021 (T.T.Y. and K.H.). T.H. is supported in part by MEXT Grant-in-Aid for Scientific Research on Innovative Areas (No.20105003) and SPIRE (Strategic Program for Innovative REsearch) Field 5. This work was supported by World Premier International Research Center Initiative (WPI Initiative), MEXT, Japan.

## References

- 1) M. Bolz, W. Buchmuller and M. Plumacher, Phys. Lett. B **443** (1998) 209 [arXiv:hep-ph/9809381].
- 2) M. Fukugita and T. Yanagida, Phys. Lett. B **174** (1986) 45.
- 3) ATLAS NOTE, ATLAS-CONF-2011-163.
- 4) CMS Physics Analysis Summary, HIG-11-032.
- 5) J. L. Evans, M. Ibe and T. T. Yanagida, Phys. Lett. B **705** (2011) 342 [arXiv:1107.3006 [hep-ph]]; J. L. Evans, M. Ibe, S. Shirai and T. T. Yanagida, arXiv:1201.2611 [hep-ph].
- 6) M. Endo, K. Hamaguchi, S. Iwamoto and N. Yokozaki, Phys. Rev. D **84** (2011) 075017 [arXiv:1108.3071 [hep-ph]]; arXiv:1112.5653 [hep-ph]; J. L. Evans, M. Ibe and T. T. Yanagida, arXiv:1108.3437 [hep-ph].
- 7) E. Halkiadakis, talk presented at CERN PH-LHC seminar, 2012.
- 8) W. Buchmuller, K. Hamaguchi, M. Ibe and T. T. Yanagida, Phys. Lett. B **643** (2006) 124 [arXiv:hep-ph/0605164].
- 9) M. Ratz, K. Schmidt-Hoberg and M. W. Winkler, JCAP **0810** (2008) 026 [arXiv:0808.0829 [hep-ph]]; J. Pradler and F. D. Steffen, Nucl. Phys. B **809** (2009) 318 [arXiv:0808.2462 [hep-ph]].
- 10) F. Iocco, G. Mangano, G. Miele, O. Pisanti and P. D. Serpico, Phys. Rept. **472**, 1 (2009) [arXiv:0809.0631 [astro-ph]].
- 11) K. Hamaguchi, T. Hatsuda and T. T. Yanagida, arXiv:hep-ph/0607256.
- 12) G. Zweig, Science **201** (1978) 973.
- 13) B. L. Ioffe, L. B. Okun, M. A. Shifman and M. B. Voloshin, Acta Phys. Polon. B **12** (1981) 229.
- 14) M. Fairbairn, A. C. Kraan, D. A. Milstead, T. Sjostrand, P. Z. Skands and T. Sloan,

- Phys. Rept. **438** (2007) 1 [hep-ph/0611040].
- 15) K. Hamaguchi, T. Hatsuda, M. Kamimura, Y. Kino and T. T. Yanagida, Phys. Lett. B **650** (2007), 268, hep-ph/0702274.
  - 16) M. Kamimura, Y. Kino and E. Hiyama, Prog. Theor. Phys. **121** (2009) 1059.
  - 17) E. Hiyama, Y. Kino and M. Kamimura, Prog. Part. Nucl. Phys. **51** (2003), 223.
  - 18) M. Kamimura, AIP Conf. Proc. **181** (1989), 330.
  - 19) M. Kamimura, Muon Catalyzed Fusion **1** (1987), 333.
  - 20) E.A. Vesman, Soviet Phys. JETP Lett. **5** (1967), 91.
  - 21) M. Ahlers, J. Kersten and A. Ringwald, JCAP **0607** (2006) 005 [hep-ph/0604188].
  - 22) B. C. Allanach, M. Battaglia, G. A. Blair, M. S. Carena, A. De Roeck, A. Dedes, A. Djouadi and D. Gerdes *et al.*, Eur. Phys. J. C **25** (2002) 113 [hep-ph/0202233].
  - 23) [CMS Collaboration], CMS-PAS-EXO-11-022.